Published in final edited form as:
Langmuir. 2010 March 2; 26(5): 3433–3440. doi:10.1021/la903267x.

Probing Orientation and Conformation of α-Helix and β-Strand Model Peptides on Self-Assembled Monolayers Using Sum Frequency Generation and NEXAFS Spectroscopies

Tobias Weidner, **Julia S. Apte**, **Lara J. Gamble**, and **David G. Castner***
National ESCA and Surface Analysis Center for Biomedical Problems, Departments of Bioengineering and Chemical Engineering, Box 351750, University of Washington, Seattle, Washington 98195

Abstract

The structure and orientation of amphiphilic α-helix and β-strand model peptide films on self-assembled monolayers (SAMs) have been studied with sum frequency generation (SFG) vibrational spectroscopy and near edge X-ray absorption fine structure (NEXAFS) spectroscopy. The α-helix peptide is a 14-mer and the β-strand is a 15-mer of hydrophilic lysine and hydrophobic leucine residues with hydrophobic periodicities of 3.5 and 2, respectively. These periodicities result the leucine side chains located on one side of the peptides and the lysine side chains on the other side. The SAMs were prepared from assembly of either carboxylic acid or methyl terminated alkyl thiols onto gold surfaces. For SFG studies the deuterated analog of the methyl SAM was used. SFG vibrational spectra in the C-H region of air dried peptides films on both SAMs exhibit strong peaks near 2965 cm^{-1}, 2940 cm^{-1} and 2875 cm^{-1} related to ordered leucine side chains. The orientation of the leucine side chains was determined from the phase of these features relative to the non-resonant gold background. The relative phase for both the α-helix and β-strand peptides showed that the leucine side chains were oriented away from the carboxylic acid SAM surface and oriented towards the methyl SAM surface. Amide I peaks observed near 1656 cm^{-1} for the α-helix peptide confirm that the secondary structure is preserved on both SAMs. A strong linear dichroism related to the amide π* orbital at 400.8 eV was observed in the nitrogen K-edge NEXAFS spectra for the adsorbed β-strand peptides, suggesting that the peptide backbones are oriented parallel to the SAM surface with the side-chains pointing towards or away from the interface. For the α-helix the dichroism of the amide π* is significantly weaker, probably due to the broad distribution of amide bond orientations in the α-helix secondary structure.

1 Introduction

Understanding the interaction of proteins and peptides with engineered surfaces from first principles is essential for the design of biomaterials for use in antifouling, implant technology and immunosensors applications.[1,2] Controlled immobilization of peptides onto artificial biointerfaces plays a key role in these technologies and it is of crucial importance to develop tools to examine interfacial properties of adsorbed peptides such as chemical composition, orientation, and secondary structure.[3–6] Since proteins bound to interfaces are complicated systems, it is helpful to investigate model systems with reduced complexity to understand the basic interaction principles. Designed peptides on well defined model surfaces more readily allow identification of adsorption binding sites and investigation of how the substrate surface properties affects the adsorbed peptide structural features.

*Corresponding author: David G. Castner, castner@nb.engr.washington.edu 1-206-543-8094 (phone).

Amphiphilic model peptides comprised of hydrophobic leucine (L) and hydrophilic lysine (K) side-chains have been successfully used as model peptides in this context.[7,8] Depending on the hydrophobic periodicity of the amino acid sequence, α-helix and β-strand peptide structures can be made with the hydrophobic side-chains on one side and the hydrophilic on the other. While model LK peptides have been studied in solution and at the air/water interface for more than a decade,[7,9–12] only a small number of adsorption studies on solid surfaces have been reported,[13–15] and only very few different surface chemistries have been investigated. The first sum frequency generation (SFG) vibrational spectroscopy studies of LK peptide adsorption were done on hydrophobic fluorocarbon and hydrophilic silica surfaces.16 This initial study was followed by an investigation of LK peptide adsorption onto hydrophobic polystyrene and hydrophilic silica surfaces using atomic force microscopy (AFM), quartz crystal microbalance (QCM) measurements and SFG vibrational spectroscopy.17 SFG, owing to its intrinsic surface sensitivity, is a powerful tool for elucidating peptide molecular scale structures at interfaces. Recently, SFG was used to study the effect of amino acid composition and sequence, chain length and ionic strength of the solvent on the orientation and secondary structure of LK peptides at polystyrene and silica surfaces.[17–19] We have also recently used X-ray photoelectron spectroscopy (XPS) and time-of-flight secondary ion mass spectrometry (ToF-SIMS) to investigate the adsorption of α-helix and β-strand LK peptides onto carboxylic acid and methyl terminated self-assembled monolayers (SAMs).20

SAMs are a versatile platform for preparing chemically well-defined model surfaces with a 2D polycrystalline structure.[21–25] SAMs are widely used to tailor the biological response towards surfaces. Well known applications include protein resistance films[26–30] as well as surfaces for specific immobilization of peptides and proteins.[6,31–34] In the context of this work, SAMs bearing nonpolar methyl (dodecane thiol, DoDT) and polar carboxylic acid (mercaptoundecanoic acid, MUDA) tail groups provide well-defined hydrophilic and hydrophobic model surfaces for the adsorption of the amphiphilic LK peptides. The α-helix model LK peptide was a 14-mer with a leucine periodicity of 3.5 ($LK\alpha_{14}$). The β-strand LK peptide was a 15-mer with a leucine periodicity of 2 ($LK\beta_{15}$). We have recently reported an initial joint SFG and solid state NMR study on the side chain dynamics of $LK\alpha_{14}$ on MUDA surfaces.[35]. In this work we presented a detailed structural characterization of dried peptide films adsorbed onto the SAMs using by SFG vibrational spectroscopy in air and near-edge X-ray absorption fine structure (NEXAFS) spectroscopy in vacuum.

2 Experimental Section

Sample preparation

Details of the procedures used to prepare the SAMs on gold substrates, synthesize the LK peptides and adsorb the LK peptides onto the SAM surfaces have been reported previously.[20] Briefly, pieces of silicon wafers (Silicon Valley Microelectronics, Inc., San Jose) were coated with 10-nm Cr and 80-nm Au (99.99%) by electron beam evaporation. Then self-assembled monolayers were prepared from DoDT, perdeuterated DoDT (d-DoDT) and MUDA (Aldrich) using 1 mM, 1mM, and 0.5 mM ethanolic solutions, respectively. The LK peptides were synthesized on a PS3 solid-state peptide synthesizer (Rainin) on a Leu-Wang resin (Novabiochem). The final peptide sequences were Ac-LKKLLKLLKKLLKL-OH for $LK\alpha_{14}$ and Ac-LKLKLKLKLKLKLKL-OH for $LK\beta_{15}$. The peptides were dissolved at twice the desired final concentration in degassed water. Phosphate buffered saline (PBS) 10× solution from Omnipur (EMD), was used to make 1× and 2× PBS solutions (137 mM NaCl, 3 mM KCl, 10 mM phosphate salts at 1×, pH ~7.4) that were degassed before use. SAM surfaces were equilibrated under the 2× PBS for 20 minutes at 37° C before addition of the 2× peptide solution. Adsorption was carried out for 2 hours at 37° C. Rinsing was done by dilution displacement with 1× PBS buffer followed by sequential one-minute rinses

in stagnant 1× buffer, stirred buffer, and 3 stirred water beakers. Samples were allowed to air-dry and then stored under nitrogen if not immediately analyzed. Peptide solution concentrations used to prepare samples for the SFG and NEXAFS experiments were 0.5 mg/mL LKα_{14} (DoDT SAMs), 0.05 mg/mL LKα_{14} (MUDA SAMs), 0.3 mg/mL LKβ_{15} (DoDT SAMs) and 0.05 mg/mL LKβ_{15} (MUDA) SAMs. The measured XPS compositions show solution concentrations of ~0.3 mg/mL produce monolayer coverage of both LK peptides on the DoDT SAMs and solution concentrations of ~0.002 mg/mL produce monolayer coverage of both LK peptides on the MUDA SAMs.[20] Significant variability in peptide coverage, both spot-to-spot on a given replicate and replicate-to-replicate, was observed for both LK peptides adsorbed onto the DoDT SAMs, but not when they were adsorbed onto the MUDA SAMs. Thus, the experimental conditions used to prepare the adsorbed peptide samples for SFG and NEXAFS analysis should result in approximately monolayer coverage on the DoDT SAMs and at least monolayer coverage on the MUDA SAMs.

SFG Setup and Data Acquisition

The SFG spectra were obtained by overlapping visible and tunable IR laser pulses (25 ps) in time and space at incidence angles of 60° and 54°, respectively. The visible beam with a wavelength of 532 nm was delivered by an EKSPLA Nd:YAG laser operating at 50 Hz, which was also used to pump an EKSPLA optical parametric generation/amplification and difference frequency unit based on barium borate and $AgGaS_2$ crystals to generate tunable IR laser radiation from 1000–4000 cm^{-1}. The bandwidth was 1 cm^{-1} for the visible pump pulses and 1 – 6 cm^{-1} for the IR laser radiation (1 cm^{-1} for 2750 – 3000 cm^{-1} and 6 cm^{-1} for higher and lower wave numbers). Both beams were unfocussed and had a diameter of approximately 3 mm at the sample. The energy for both beams was 160 μJ per pulse. These experimental conditions have been shown not to cause visible damage to the Au or SAM.[30] The SFG signal generated at the sample was then analyzed by filters and a monochromator, detected with a gated photomultiplier tube and stored in a computer. The spectra were collected with 400 shots per data point in 1 to 4 cm^{-1} increments. All spectra were recorded in the ppp (sum, visible, and infrared) polarization combination. Because of the Fresnel coefficients of metals surfaces, the x- and y-component contributions of the IR electric field at the surface are smaller than the z-component.36 Consequently, the SF generation is more intense when using a polarization combination with a perpendicular component (i.e. ssp, or ppp). Since the ppp polarization combination probes a greater number of combinations of tensor elements that can either constructively or destructively interfere, it often generates a larger signal value on metallic surfaces than the ssp polarization combination.36–38 All spectra were recorded in ppp (sum, visible, and infrared) polarization combination. The SFG spectra were normalized by a spectrum of a d-DoDT self-assembled monolayer on gold.

The fitting routine for the SFG data[39] used the following expression for the SFG intensity:[40]

$$I_{SFG} \propto |\chi^{(2)}|^2 = \left| \chi^{(2)}_{NR} e^{i\phi} + \sum_{\nu} \int_{-\infty}^{\infty} \frac{A_\nu e^{i\phi_\nu} e^{-[\omega_L - \omega_\nu/\Gamma_\nu]^2}}{\omega_{IR} - \omega_L + i\Gamma_L} d\omega_L \right|^2 \quad [1]$$

Here, $\chi^{(2)}_{NR}$ is the second order nonlinear susceptibility of the nonresonant background, A_ν is the strength of the ν th vibrational mode, ϕ denotes the phase of the respective mode and ω_{IR} refers to the frequency of the incident IR field. The integral is over Lorentzian lines, centered at ω_L with a width Γ_ν, having a Gaussian distribution. The Lorentzian line widths were set to 2 cm^{-1} and Γ_ν was allowed to vary since the two contributions to the total line width could not be separated within the accuracy of the measurements. Phase values are reported as relative values to the nonresonant gold background and identical phases were

assumed for all methyl and methylene related stretches to limit the number of independent parameters. Releasing these fitting constraints did not significantly change the resonance positions or phases.

Near-Edge X-ray Absorption Fine Structure Spectroscopy

NEXAFS spectra were taken at the National Synchrotron Light Source (NSLS) U7A beamline at Brookhaven National Laboratory, using an elliptically polarized beam with ~85% p-polarization. This beam line uses a monochromator and 600 l/mm grating that provides a full-width at half-maximum (FWHM) resolution of ~0.15 eV at the carbon K-edge (285 eV). The monochromator energy scale was calibrated using the 285.35 eV C 1s − π* transition on a graphite transmission grid placed in the path of the X-rays. To eliminate the effect of incident beam intensity fluctuations and monochromator absorption features, nitrogen K-edge NEXAFS spectra were normalized by the signal from a bare SAM monolayer (both methyl and carboxylic-acid terminated monolayers) and dividing both signals by the beam flux (I_{ring}) during each respective data acquisition, (EY_{sample}/ $I_{ring\text{-}sample}$)*($I_{ring\text{-}control}$/$EY_{control}$). Partial electron yield was monitored by a detector with the bias voltage maintained at −360 V for the nitrogen K-edge spectrum. Samples were mounted to allow rotation about the vertical axis to change the angle between the sample surface and the incident X-ray beam. The NEXAFS angle is defined as the angle between the incident X-ray beam and the sample surface.

3 Results

3.1 Sum Frequency Generation Spectroscopy

Figure 1 shows the expected orientations of $LK\alpha_{14}$ and $LK\beta_{15}$ on the MUDA and DoDT SAMs (the leucine side chains interacting with the DoDT surface and the lysine side chains interacting with the MUDA surface). Figure 2 and Figure 3 show the SFG spectra in the CH stretching regions for $LK\alpha_{14}$ and $LK\beta_{15}$ peptides adsorbed onto the MUDA and d-DoDT SAMs. The solid lines are the least-square fits of the SFG data to eq 1. The strong peaks between 2800 and 3000 cm^{-1} in all the spectra are assigned to CH resonances of the peptides[17,41] and the underlying MUDA SAM.[42,43] On d-DoDT only peptide related CH stretching modes are observed. In addition, $LK\alpha_{14}$ adsorbed onto the MUDA SAM exhibited a NH stretching resonance around 3300 cm^{-1} (data not shown).[44,45] The assignment for this NH mode is not straightforward and it has been assigned to the N-terminus of the lysine side chains as well as amide A modes of the NH moieties in the α-helical peptide backbone.[17−19,46] In a separate SFG study using ^{15}N isotope labels on the terminal amine group in the lysine side chains this feature was unequivocally assigned to a stretching mode of the terminal amine.[47] The peptide films adsorbed onto the DoDT SAM also show weak traces of OH stretching modes near 3190 cm^{-1} associated with tetrahedrally coordinated hydrogen bonded water molecules (data not shown).[17,48] The two lower spectra in Figure 2 ($LK\alpha_{14}$ and $LK\beta_{15}$ adsorbed onto MUDA) exhibit five peaks associated with the adsorbed peptides. Three of these peaks arise from the terminal methyl groups on the peptide leucine side chains: the CH_3 symmetric stretch near 2875 cm^{-1} , the CH_3 Fermi resonance near 2941 cm^{-1} and the CH_3 asymmetric stretch near 2965 cm^{-1} .[41,49] The methylene Fermi resonance near 2890 cm^{-1} and the asymmetric methylene stretch near 2907 could be from either the methylene units in the leucine or lysine side chains.[17,41] The CH_3 SFG signal is phase shifted by nearly π/2 relative from the Au substrate signal (see Table 1). Ward et al. have shown earlier, that the phase of a methyl related resonance relative to the phase of the non-resonant gold background is correlated to the methyl orientation.[50] A relative phase of ≈π/2 has been observed for alkanethiol SAMs on gold with methyl units point away from the surface. We thus conclude that the hydrophobic leucine side chains in both the α-helix and the β-strand peptides are oriented away from the charged

COOH terminated interface on MUDA. Note that the ability to do this orientational analysis is a significant advantage of using gold substrates compared to dielectric and polymer substrates, where measuring the phase of SFG signals can be challenging.

The CH region SFG spectra of $LK\alpha_{14}$ and $LK\beta_{15}$ adsorbed onto d-DoDT SAMs shown in Figure 3 exhibit pronounced features related to the methyl groups of the leucine side chains.[17,41] The symmetric CH_3 stretch can be found near 2873 cm^{-1} , the asymmetric CH_3 stretch is located at around 2962 cm^{-1}, and the CH_3 Fermi resonance is seen near 2935 cm^{-1}. There are no traces of methylene stretching modes in these spectra, which indicates either an all-trans conformation of the aliphatic chains or a completely disordered configuration. The former possibility is more likely – at least for the leucine chains – in view of the observed methyl modes.[42] Most importantly, the resonances are almost in phase with the nonresonant gold background (see Table 1). This means the methyl units of the leucine side chains are oriented towards the hydrophobic interface.[50]

Figure 4 summarizes the intensity ratios of the symmetric to the asymmetric methyl stretching modes for the peptides adsorbed onto the MUDA and DoDT SAMs. These values can be used for orientation analysis. Tilt angles can be calculated from these values if distribution of tilt angles is known.[51,52] Although the distribution of tilt angles is not known for the samples in this study, the peak intensity ratio still provides important qualitative information about the alignment of the leucine methyl groups. The $LK\beta_{15}$ symmetric/asymmetric ratios are 2–3 times higher than the $LK\alpha_{14}$ symmetric/asymmetric ratios on both surfaces, which suggests the leucine side chains in the $LK\beta_{15}$ adsorbed peptides are either more aligned along the surface normal or have at least a narrower distribution of tilt angles.[51] Both possibilities are likely given the structural differences between the $LK\alpha_{14}$ and $LK\beta_{15}$ peptides.[20]

SFG can also provide information about how peptide adsorption affects the underlying SAMs. The d-DoDT SAM is especially well suited for such an analysis because the peptide CH stretches and the SAM CD stretches are well separated. The SFG spectra of pristine and peptide covered d-DoDT SAMs in the CD region are shown in Figure 5. CD_3 stretching modes are clearly visible in the spectra. The pristine SAM spectrum exhibits the asymmetric and symmetric CD_3 stretching modes and the CD_3 Fermi resonance at 2223 cm^{-1}, 2128 cm^{-1} and 2071 cm^{-1} , respectively. There are no spectral features related to the deuterated methylene chains visible in this spectrum, indicating that the SAM is predominantly in an all-trans conformation. In the spectra of the peptide covered SAMs the intensity of the symmetric stretching mode was somewhat lower and the asymmetric stretching resonance decreased to the noise level. In addition, there are no resonances related to gauche defects in the aliphatic chains visible in the spectra, suggesting that the d-DoDT SAMs maintained an all-trans conformation after peptide adsorption. This indicates that the peptide side chains did not penetrate into the SAM, as this would likely result in the formation of gauche defects in the SAM structure. The intensity reduction for the symmetric peak is likely caused by slightly decreased order within the top methyl layer of the SAM due to interactions with the peptide overlayer. The dramatic decrease of the asymmetric stretching mode at 2223 cm^{-1} is surprising. Since the SFG intensity ratio of symmetric and asymmetric modes of the terminal methyl groups is related to the molecular orientation and the distribution width of tilt angles, the decease of the asymmetric resonance could be explained by a reorientation of the terminal methyl species of the d-DoDT SAM to maximize hydrophobic interactions with the leucine side chains on the peptides. This trend can be further quantified by methyl tilt angle estimations based on published procedures employing the symmetric/asymmetric peak ratios.[53] The tilt angle of the methyl group relative to the surface normal in the pristine SAM was calculated to be ca. 27°, in reasonable agreement with literature data for hydrogenated dodecanethiols on gold.[53] Since the intensity of the asymmetric mode is below the detection

limit for the peptide-covered films, the tilt angle can only be estimated to be lower than ca. 10°.

The structure of DoDT SAMs after soaking in PBS at 37° C for two hours either with or without the presence of $LK\alpha_{14}$ was also investigated. The SFG spectra after these treatments along with a pristine DoDT spectrum are shown in Figure 6. The pristine DoDT spectrum exhibits only the methyl related stretches expected for highly ordered alkanethiol SAMs in an all-trans configuration. In contrast, significant intensity of the methylene modes was detected after soaking the DoDT SAM in pure PBS. Also, the intensity of the methyl resonances decreased significantly. This is indicative of a poorly ordered film with a large number of trans-gauche defects.[42,54] Presumably the buffer penetrates into the film and disturbs the lateral order of the aliphatic chains. This is consistent with XPS detecting oxygen and ToF-SIMS detecting H_3O^+ secondary ions from DoDT SAMs exposed to buffer.[20] Conversely, with LK peptides present in the solution during the immersion of the SAM substrate, no methylene stretching vibrations (i.e. no gauche defects) are detectable in the spectrum (Figure 6). This suggests the interactions between the peptide and the DoDT SAM exclude water from the interface and protect the film from becoming disordered by contact with buffer.

A well established method to obtain information about the secondary structure of peptides at interfaces is to examine the amide I region of the SFG spectrum.[55] This region corresponds to the backbone C=O stretching mode which is weakly coupled with the N-H and the C-N bond stretches. The position of the amide I signal has been shown to be sensitive to the secondary structure of peptides.[56–58] SFG spectra acquired in the amide I region (1550–1750 cm^{-1}) for the $LK\alpha_{14}$ and $LK\beta_{15}$ peptides on MUDA and DoDT SAMs are shown in Figure 7. The $LK\alpha_{14}$ peptide showed a clear amide I signal when adsorbed onto the MUDA SAM. The intensity of the amide I signal was weaker when the $LK\alpha_{14}$ peptide was adsorbed onto the DoDT SAM. In both cases the amide I peak positions were near 1655 cm^{-1}, the characteristic value for α-helical structures.[56–58] The presence of a measurable amide I signal from the adsorbed $LK\alpha_{14}$ peptides indicates that these helical structures have amide bond orientations where the dipoles of the carbonyl groups do not cancel out. The amide I SFG spectrum of the $LK\beta_{15}$ peptides did not have a detectable SFG peak in the amide I region when adsorbed onto the MUDA or DoDT SAMs. β-sheet amide I peaks are expected to be located between ~1630 cm^{-1} and 1680 cm^{-1} .[55] The lack of an amide I signal for the adsorbed $LK\beta_{15}$ peptides can be explained by a symmetric placement of the backbone carbonyls in that structure. Thus the $LK\beta_{15}$ would be SFG inactive due to the C=O dipoles offsetting one another. This effect has also been observed for $LK\beta_7$ peptides (β-sheet LK peptides with 7 residues) on fluorocarbon surfaces.[16]

3.2 NEXAFS Spectroscopy

NEXAFS spectra provide complementary information about the electronic structure of the sample. They exhibit characteristic absorption resonances corresponding to the electronic transition from a given core level to unoccupied molecular orbitals. These features can be used to detect the presence of representative molecular moieties at surfaces, as well as their orientation/order.

The N *K*-edge spectra of $LK\alpha_{14}$ and $LK\beta_{15}$ on DoDT and MUDA SAMs recorded at incident X-ray angles of 70° and 20° are presented in Figure 8 and Figure 9. All spectra in these figures exhibit the characteristic N 1s – continuum adsorption excitation and a series of absorption resonances characteristic of the adsorbed peptides, namely a sharp π* resonance near 400 eV, a relatively broad σ* transition near 411 eV related to the amide bond, and another broad σ* feature near 406 eV assigned to overlapping N-C and N-H orbitals.59–64 Although all spectra have the same resonances, the relative intensities of

some resonances do vary. These intensity differences are likely due to variations in peptide packing or molecular conformation. A fingerprint of LK peptide orientation and order on the two SAM surfaces is given by the linear dichroism in the NEXAFS spectra, i.e. the dependence of the intensity of the resonances on the incidence angle of X-ray light. This is because the cross section of the resonant photoexcitation process depends on the orientation of the electric field vector of the incident synchrotron light with respect to the transition dipole moment (TDM) of the molecular orbital under study.[65] For ordered films, the intensity of the absorption resonance changes with variation of the X-ray incidence angle. A convenient way to monitor the linear dichroism is the difference between the spectra acquired at near-normal (70°) and grazing (20°) incidence. Such difference spectra are also shown in Figure 8 and Figure 9 for absorption at the nitrogen *K*-edge on both the DoDT and MUDA SAMs for the α-helix (Figure 8) and the β-strand (Figure 9). For $LK\alpha_{14}$ the dichroism of the amide π* is weak and, consequently, no pronounced difference peaks are visible in the "70°"–"20°" curve. This suggests a low orientational order of the amide bond for the adsorbed $LK\alpha_{14}$ peptide. This is not surprising in view of the broad distribution of amide bond orientation angles in the helical structure of the $LK\alpha_{14}$ peptide. An average over the peptide bonds only results in a small net transition dipole moment along the long axis of the helix. For $LK\beta_{15}$ the characteristic π* and σ* resonances vary noticeably upon alteration of the X-ray incidence angle, which is highlighted by the peaks in the difference spectra (Figure 9, bottom). Since the amide π* orbitals are oriented perpendicular to the amide bond, the observed intensity differences indicate that the $LK\beta_{15}$ peptide is adsorbed onto the SAMs in a conformation with its backbone parallel and its side-chains pointing towards and away from the DoDT and MUDA surfaces.

4 Discussion

From the characteristic stretching modes related to $LK\alpha_{14}$ and $LK\beta_{15}$ peptides that are observed in the SFG spectra it can be concluded that the peptides were adsorbed onto the SAM surfaces. The peptides appear to form densely packed layers as the intensities of the peptide C-H vibration modes are comparable to those observed for alkanethiol SAMs on gold, well known to form densely packed organic films on Au surfaces.[21–23,66] This is all consistent with XPS and ToF-SIMS studies that show near saturation coverage of the adsorbed peptides is obtained from the peptide solution concentrations used to prepare the samples for SFG and NEXAFS experiments.[20] The chemical integrity of the peptides is evident from the NEXAFS data where all the expected features could be observed in the N *K*-edge spectra.[59–64] This is also consistent with the previous XPS and ToF-SIMS results.[20]

The β-strand secondary structure of $LK\beta_{15}$ is preserved on both SAMs and the adsorbed peptides form ordered structures. This can be concluded from the linear dichroism observed for the amide-related resonances in the NEXAFS spectra. The linear dichroism is most pronounced on the MUDA SAM and suggests that the backbone of the β-strands are oriented predominantly parallel to the surface.[65] The lack of an SFG amide I signal further supports this view. SFG signal from β-sheet structures is usually generated at β-turn sites. Well-ordered β-strand structures on the other hand lack turn sites. That along with the symmetric structure of the CO groups in ordered layers results in canceling of the SFG amide I signal due to offsetting C=O group orientations.[56]

The SFG spectra of $LK\alpha_{14}$ adsorbed onto the MUDA and DoDT SAMs both exhibit an amide I SFG signal near 1655 cm^{-1}. This resonance is commonly related to intact helical structures in adsorbed peptides and proteins.[17–19,67] Thus, it can be concluded that the $LK\alpha_{14}$ peptide maintains its α-helical structure when adsorbed onto these surfaces. However, the intensity of the amide I peak for $LK\alpha_{14}$ adsorbed onto the DoDT SAM is weaker than the amide I peak for $LK\alpha_{14}$ adsorbed onto the MUDA SAM. Possible

explanations for this observation include a portion of the adsorbed peptides assuming a random coil configuration on the DoDT SAM, a lower peptide coverage on the DoDT SAM, a laterally more disordered film on the DoDT SAM, or different orientations on the two surface. The latter possibility is less likely in view of the similarities in the CH SFG spectra. The weak linear dichroism observed for the amide-related resonances in the NEXAFS spectra for the $LK\alpha_{14}$ peptide adsorbed onto both MUDA and DoDT is thus largely due to the broad distribution of CO bond orientations inherent to the α-helical configuration, although disorder within the adsorbed peptide film on the DoDT SAM could also contribute to the weak linear dichroism observed from that sample.

The C-H SFG spectra are very similar for both α-helix and β-strand peptide films and are dominated by peaks characteristic of their leucine side chains. The only noticeable variation in the CH spectra is the higher ratio of the symmetric to asymmetric CH_3 stretching modes in the $LK\beta_{15}$ spectra related to a more upright orientation or a narrower distribution of orientations of the leucine side chains.[51,52] This is most likely an effect of the inherently more aligned leucine side chains in β-strand structures as compared to α-helices.[20] However, there are significant differences in the SFG data for the two different SAM substrates (e.g., the phase of the methyl stretches). This suggests that the leucine side chain orientation is mostly driven by the chemistry of the SAM-peptide interaction.

On DoDT surfaces, according to the phase of the related SFG resonances, the leucine side chains are oriented towards the peptide-SAM interface. This observation is consistent with bonding occurring via hydrophobic interactions of the leucine methyl groups with the DoDT surface. This analysis is in good agreement with earlier *in situ* SFG studies of LK peptides at hydrophobic fluorocarbon and polystyrene surfaces, where the signature of ordered leucine species was considered as an evidence of hydrophobic leucine-surface interactions.[16–19] However, the side chain orientation with respect to the interface could not be confirmed in those studies since the fluorocarbon and polystyrene surfaces lack the non-resonant background signal required for the phase determination.[50,54] Hydrophobic leucine-SAM interactions are further corroborated by the observation that the presence of LK peptides at the SAM-buffer interface keeps the DoDT SAM from becoming disordered by exposure to buffer. The leucine-methyl interactions appear to inhibit the water molecules from penetrating into DoDT SAM when the peptides are present on the SAM surface. Therefore, the SAMs are more ordered than those exposed to pure buffer, although the degree of order is not as high as in the pristine SAMs.

The C-H region SFG data for MUDA surfaces also show similar spectral features for both peptides. The strong signature of the CH_3 stretches in combination with the phase of the signal reveal well aligned leucine side chains which point away from the surface. This leucine orientation is expected in a scenario where the positively charged lysine residues are oriented towards the negatively charged COOH groups of the MUDA SAM.[16,17] Interestingly, in situ SFG data reported for LK peptides in buffer at charged SiO_2 surfaces did not show discernible peaks related to ordered leucine side chains.[16–19] However, as has been previously noted for LK peptides adsorbed onto silica surfaces,[16] the drying process seems to promote the formation of ordered leucine alkane side chains that produce SFG spectra similar to alkane-based SAMs on gold.

5 Conclusion

Air-dried films of the amphiphilic model peptides $LK\alpha_{14}$ and $LK\beta_{15}$ on charged MUDA and hydrophobic DoDT SAM surfaces have been characterized using SFG and NEXAFS spectroscopies. The peptides adsorbed with intact secondary structures on both surfaces. The

orientations of the leucine side chains were similar for both secondary structures (α-helix and β-strand), but showed distinct variation with the chemistry of the substrate.

Based on the SFG spectral data and phase analysis, the charged MUDA surfaces interact with the hydrophilic lysine side chains leaving the leucine side chains pointing away from the surface. In contrast, the hydrophobic DoDT surfaces interact with the methyl groups of the leucine side chains, leaving the lysine side chains pointing away from the surface.

This investigation highlights the complementary nature of SFG and NEXAFS for determining the peptide backbone orientation in α-helix and β-strand structures. For the adsorbed $LK\alpha_{14}$ peptides, amide I peaks were readily detected by SFG while little linear dichroism in the N-*K* edge amide π* peaks were detected by NEXAFS. For the adsorbed $LK\beta_{15}$ peptides, amide I peaks were not detected by SFG while significant linear dichroism in the N-*K* edge amide π* peak was detected by NEXAFS.

Acknowledgments

The authors thank Robert Latour and Galen Collier at Clemson University for help with the peptide illustrations; Nicholas Breen, Gil Goobes and Riki Goobes at the University of Washington for support with peptide synthesis; and Pat Stayton, Lizzy Mayorga-Szott, Loren Baugh and Scott Curtin at the University of Washington for technical discussions. Financial support by the National Institute of Health grants NIH GM-074511 and NIH EB-002027 is gratefully acknowledged. We also thank Dan Fischer and Cherno Jaye for their expert technical assistance with the NEXAFS experiments. NEXAFS studies were performed at the NSLS, Brookhaven National Laboratory, which is supported by the U.S. Department of Energy, Division of Materials Science and Division of Chemical Sciences. This material is based upon work supported under a National Science Foundation Graduate Research Fellowship (J.S.A.) and a research fellowship granted by the Deutsche Forschungsgemeinschaft (T.W.).

References

1. Horbett, TA.; Brash, JL., editors. Proteins at Interfaces II: Fundamentals and Applications. Washington D. C: American Chemical Society; 1995.
2. Ratner BD. Macromolecular Symposia 1997;130:327–335.
3. Fremont DH, Matsumura M, Stura EA, Peterson PA, Wilson IA. Science 1992;257:919–927. [PubMed: 1323877]
4. Russell CJ, Thorgeirsson TE, Shin YK. Biochemistry 1996;35:9526–9532. [PubMed: 8755733]
5. Krüger P, Schalke M, Wang Z, Notter RH, Dluhy RA, Losche M. Biophys. J 1999;77:903–914. [PubMed: 10423435]
6. Castner DG, Ratner BD. Surf. Sci 2002;500:28–60.
7. DeGrado WF, Lear JD. J. Am. Chem. Soc 1985;107:7684–7689.
8. Degrado WF, Wasserman ZR, Lear JD. Science 1989;243:622–628. [PubMed: 2464850]
9. Kerth A, Erbe A, Dathe M, Blume A. Biophys. J 2004;86:3750–3758. [PubMed: 15189871]
10. Beven L, Castano S, Dufourcq J, Wieslander A, Wroblewski H. Eur. J. Biochem 2003;270:2207–2217. [PubMed: 12752440]
11. Castano S, Desbat B, Laguerre M, Dufourcq J. Biochim. Biophys. Acta 1999;1416:176–194. [PubMed: 9889361]
12. Dieudonne D, Gericke A, Flach CR, Jiang X, Farid RS, Mendelsohn R. J. Am. Chem. Soc 1998;120:792–799.
13. Long JR, Oyler N, Drobny GP, Stayton PS. J. Am. Chem. Soc 2002;124:6297–6303. [PubMed: 12033857]
14. Stewart S, Fredericks PM. Spectrochim. Acta A 1999;55:1615–1640.
15. Herne TM, Ahern AM, Garrell RL. Anal. Chim. Acta 1991;246:75–84.
16. Samuel, NT. PhD Thesis. University of Washington: 2005.
17. Mermut O, Phillips DC, York RL, McCrea KR, Ward RS, Somorjai GA. J. Am. Chem. Soc 2006;128:3598–3607. [PubMed: 16536533]

18. Phillips DC, York RL, Mermut O, McCrea KR, Ward RS, Somorjai GA. J. Phys. Chem. C 2007;111:255–261.
19. York RL, Mermut O, Phillips DC, McCrea KR, Ward RS, Somorjai GA. J. Phys. Chem. C 2007;111:8866–8871.
20. Apte JS, Collier G, Latour RA, Gamble LJ, Castner DG. Langmuir. 2009 submitted.
21. Ulman, A. Self-Assembled Monolayers of Thiols. 1 ed.. Vol. Vol. 24. San Diego: Academic Press; 1998.
22. Ulman, A. An Introduction to Ultrathin Organic Films. San Diego: Academic Press; 1991.
23. Love JC, Estroff LA, Kriebel JK, Nuzzo RG, Whitesides GM. Chem. Rev 2005;105:1103–1169. [PubMed: 15826011]
24. Schreiber F. J. Phys.: Condens. Matter 2004;16:R881–R900.
25. Leung TYB, Schwartz B, Scoles G, Schreiber F, Ulman A. Surf. Sci 2000;458:34–52.
26. Harder P, Grunze M, Dahint R, Whitesides GM, Laibinis PE. J. Phys. Chem. B 1998;102:426–436.
27. Herrwerth S, Eck W, Reinhardt S, Grunze M. J. Am. Chem. Soc 2003;125:9359–9366. [PubMed: 12889964]
28. Prime KL, Whitesides GM. Science 1991;252:1164–1167.
29. Li LY, Chen SF, Zheng J, Ratner BD, Jiang SY. J. Phys. Chem. B 2005;109:2934–2941. [PubMed: 16851306]
30. Stein MJ, Weidner T, McCrea KR, Castner DG, Ratner BD. J. Phys. Chem. B 2009;113:11550–11556. [PubMed: 19639981]
31. Ratner BD, Bryant SJ. Ann. Rev. Biomed. Eng 2004;6:41–75. [PubMed: 15255762]
32. Mrksich M, Whitesides GM. Annu. Rev. Biophys. Biomol. Struct 1996;25:55–78. [PubMed: 8800464]
33. Nam JM, Han SW, Lee KB, Liu XG, Ratner MA, Mirkin CA. Angew. Chem. Int. Ed 2004;43:1246–1249.
34. Wegner GJ, Lee NJ, Marriott G, Corn RM. Anal. Chem 2003;75:4740–4746. [PubMed: 14674449]
35. Breen NF, Weidner T, Li K, Castner DG, Drobny GP. J. Am. Chem. Soc. in press.
36. Zhang H, Romero C, Baldelli S. J. Phys. Chem. B 2005;109:15520–15530. [PubMed: 16852969]
37. Greenler RG. J. Chem. Phys 1966;44:310–314.
38. Francis SA, Ellison AH. J.Opt. Soc. Am 1959;49:131–134.
39. Moore FG, Becraft KA, Richmond GL. Appl. Spectrosc 2002;56:1575–1578.
40. Bain CD. J. Chem. Soc., Faraday Trans 1995;91:1281–1296.
41. Watry MR, Richmond GL. J. Phys. Chem. B 2002;106:12517–12523.
42. Himmelhaus M, Eisert F, Buck M, Grunze M. J. Phys. Chem. B 2000;104:576–584.
43. Asanuma H, Noguchi H, Uosaki K, Yu HZ. J. Phys. Chem. B 2006;110:4892–4899. [PubMed: 16526728]
44. Chae BLSW, Lee B, Choi W, Kim SB, Jung YM, Jung JC, Lee KH, Ree M. Langmuir 2003;19:9459–9465.
45. Krimm S, Bandekar J. Adv. Protein Chem 1986;38:181–364. [PubMed: 3541539]
46. Jung SY, Lim SM, Albertorio F, Kim G, Gurau MC, Yang RD, Holden MA, Cremer PS. J. Am. Chem. Soc 2003;125:12782–12786. [PubMed: 14558825]
47. Weidner T, Breen NF, Dobny GP, Castner DG. submitted.
48. Du Q, Freysz E, Shen YR. Phys. Rev. Lett 1994;72:238–241. [PubMed: 10056094]
49. Ji N, Shen YR. J. Chem. Phys 2004;120:7107–7112. [PubMed: 15267614]
50. Ward RN, Davies PB, Bain CD. J. Phys. Chem 1993;97:7141–7143.
51. Cimatu K, Baldelli S. J. Phys. Chem. C 2007;111:7137–7143.
52. Wang J, Buck SM, Chen Z. J. Phys. Chem. B 2002;106:11666–11672.
53. Nishi N, Hobara D, Yamamoto M, Kakiuchi T. J. Chem. Phys 2003;118:1904–1911.
54. Lambert AG, Davies PB, Neivandt DJ. Appl. Spectrosc. Rev 2005;40:103–145.
55. Singh, BR., editor. Infrared Analysis of peptides and Proteins. Vol. Vol. 750. Washington D.C: American Chemical Society; 2000.

56. Chen XY, Wang J, Sniadecki JJ, Even MA, Chen Z. Langmuir 2005;21:2662–2664. [PubMed: 15779931]
57. Chen XY, Boughton AP, Tesmer JJG, Chen Z. J. Am. Chem. Soc 2007;129:12658. [PubMed: 17902674]
58. York RL, Holinga GJ, Guyer DR, McCrea KR, Ward RS, Somorjai GA. Appl. Spectrosc 2008;62:937–940. [PubMed: 18801230]
59. Cooper G, Gordon M, Tulumello D, Turci C, Kaznatcheev K, Hitchcock AR. J. Electron. Spectrosc. Relat. Phenom 2004;137:795–799.
60. Gordon ML, Cooper G, Morin C, Araki T, Turci CC, Kaznatcheev K, Hitchcock AP. J. Phys. Chem. A 2003;107:6144–6159.
61. Zubavichus Y, Zharnikov M, Schaporenko A, Grunze M. J. Electron. Spectrosc. Relat. Phenom 2004;134:25–33.
62. Zubavichus Y, Zharnikov M, Shaporenko A, Fuchs O, Weinhardt L, Heske C, Umbach E, Denlinger JD, Grunze M. J. Phys. Chem. A 2004;108:4557–4565.
63. Zubavichus Y, Shaporenko A, Grunze M, Zharnikov M. J. Phys. Chem. B 2007;111:9803–9807. [PubMed: 17663583]
64. Zubavichus Y, Shaporenko A, Grunze M, Zharnikov M. J. Phys. Chem. A 2005;109:6998–7000. [PubMed: 16834062]
65. Stöhr, J. NEXAFS Spectroscopy. Vol. Vol. 25. Berlin: Springer-Verlag; 1992.
66. Schreiber F. Prog. Surf. Sci 2000;65:151–256.
67. Wang J, Chen XY, Clarke ML, Chen Z. J. Phys. Chem. B 2006;110:5017–5024. [PubMed: 16526745]

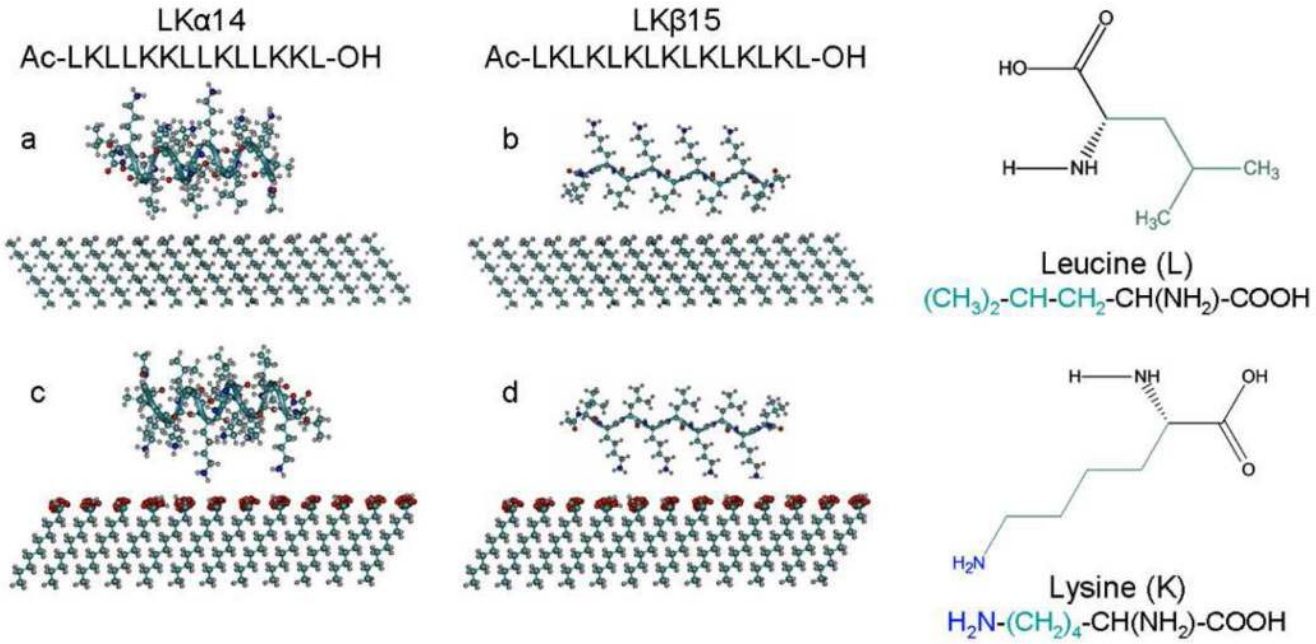

Figure 1.
Schematic drawing of the amphiphilic $LK\alpha_{14}$ and $LK\beta_{15}$ peptides interacting with the surface of a hydrophobic dodecanethiol (DoDT) SAM and a charged mercaptoundecanoic acid (MUDA) SAM.

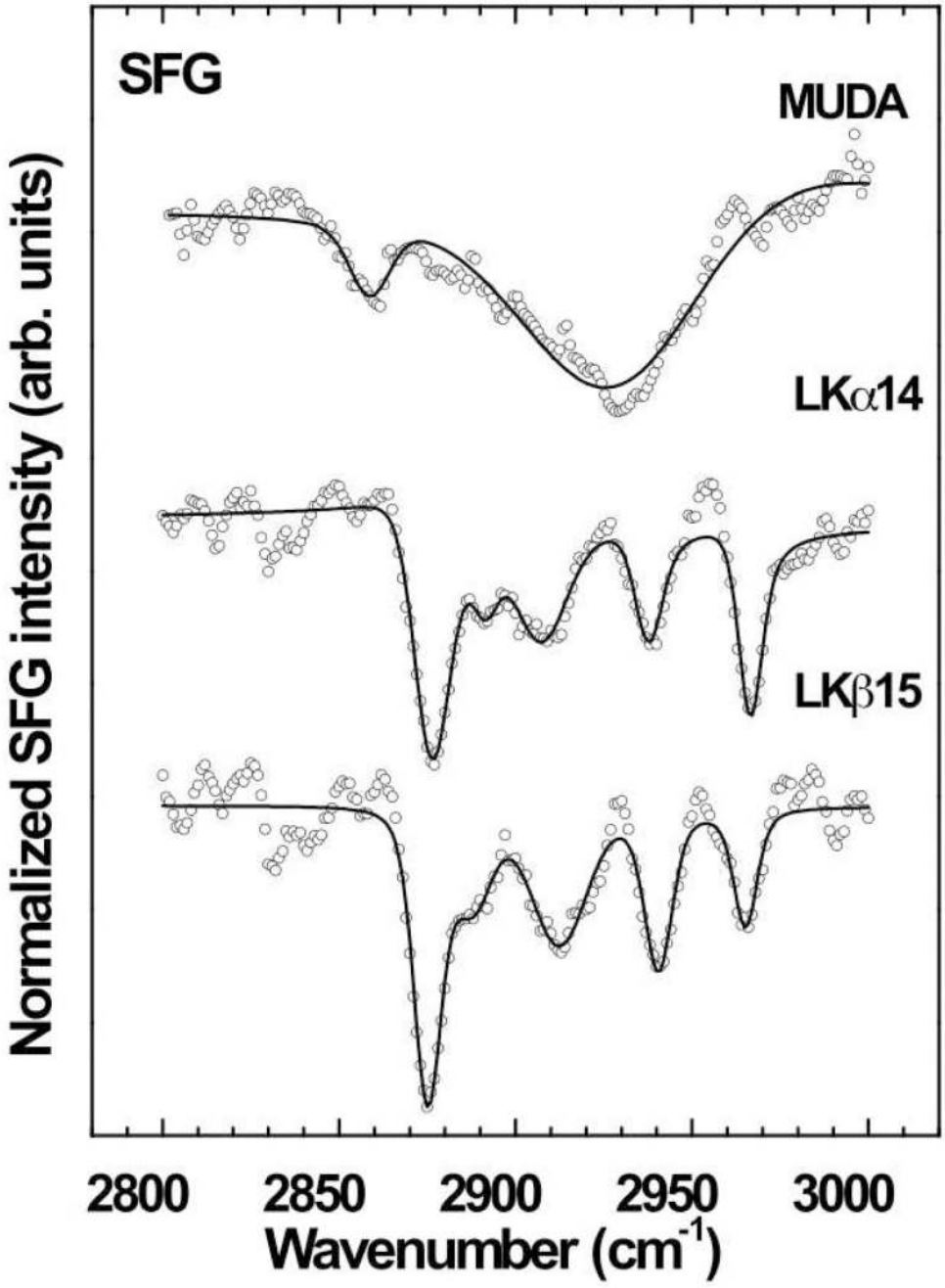

Figure 2.
SFG CH region spectra of $LK\alpha_{14}$ and $LK\beta_{15}$ peptides adsorbed onto mercaptoundecanoic acid SAMs. Strong peaks related to the methyl groups of the leucine side chains are detected. A spectrum of the plain mercaptoundecanoic acid SAM is shown as a reference.

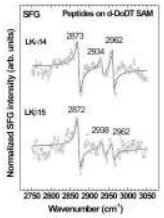

Figure 3.
SFG CH region spectra of $LK\alpha_{14}$ and $LK\beta_{15}$ peptides adsorbed onto deuterated dodecanethiol SAMs. Resonances related to the methyl groups of the leucine side chains are detected.

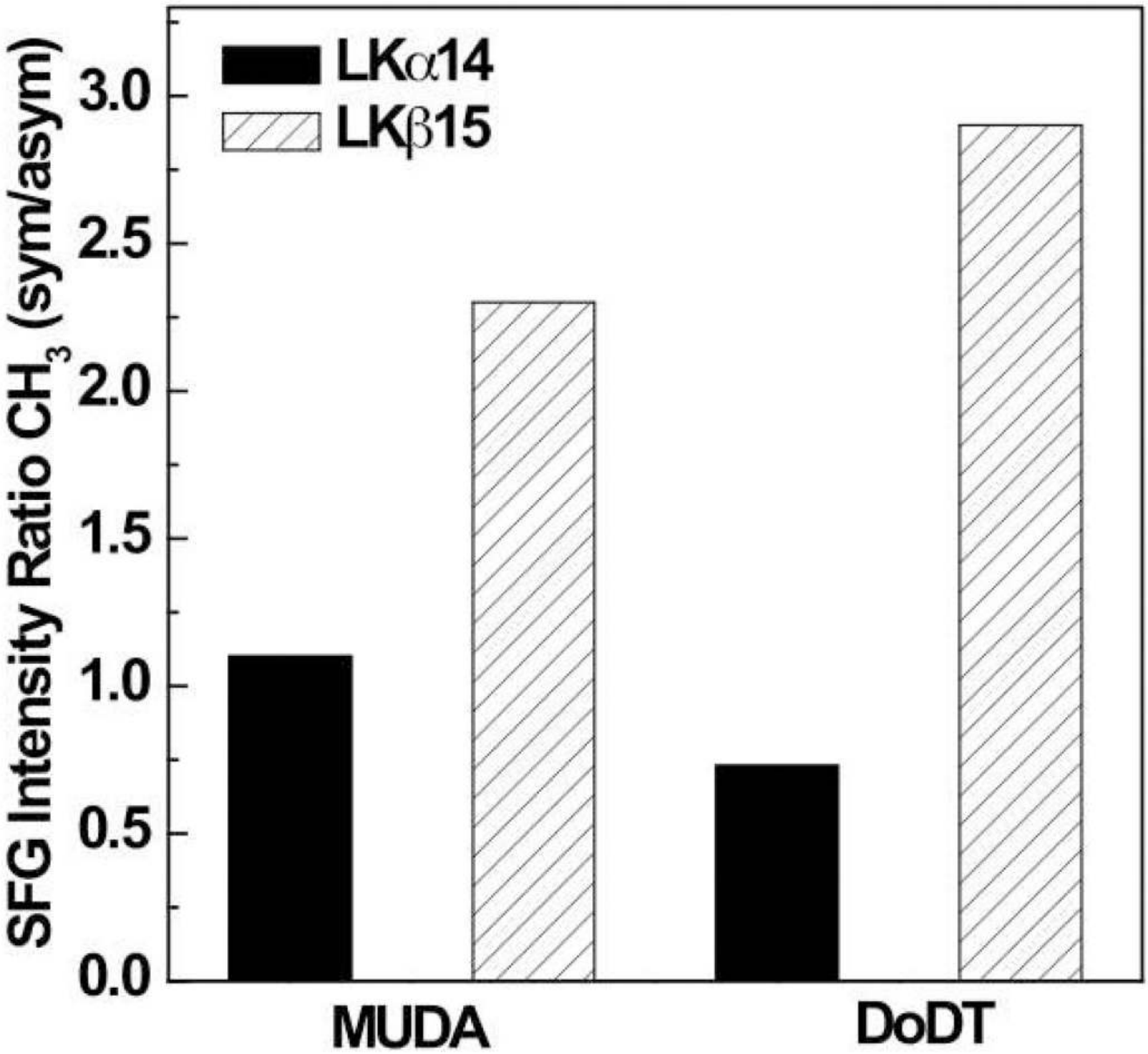

Figure 4.
SFG spectral analysis for the LK peptides adsorbed onto MUDA and DoDT SAMs. The intensity ratio of the CH_3 symmetric stretch to the CH3 asymmetric stretch are displayed.

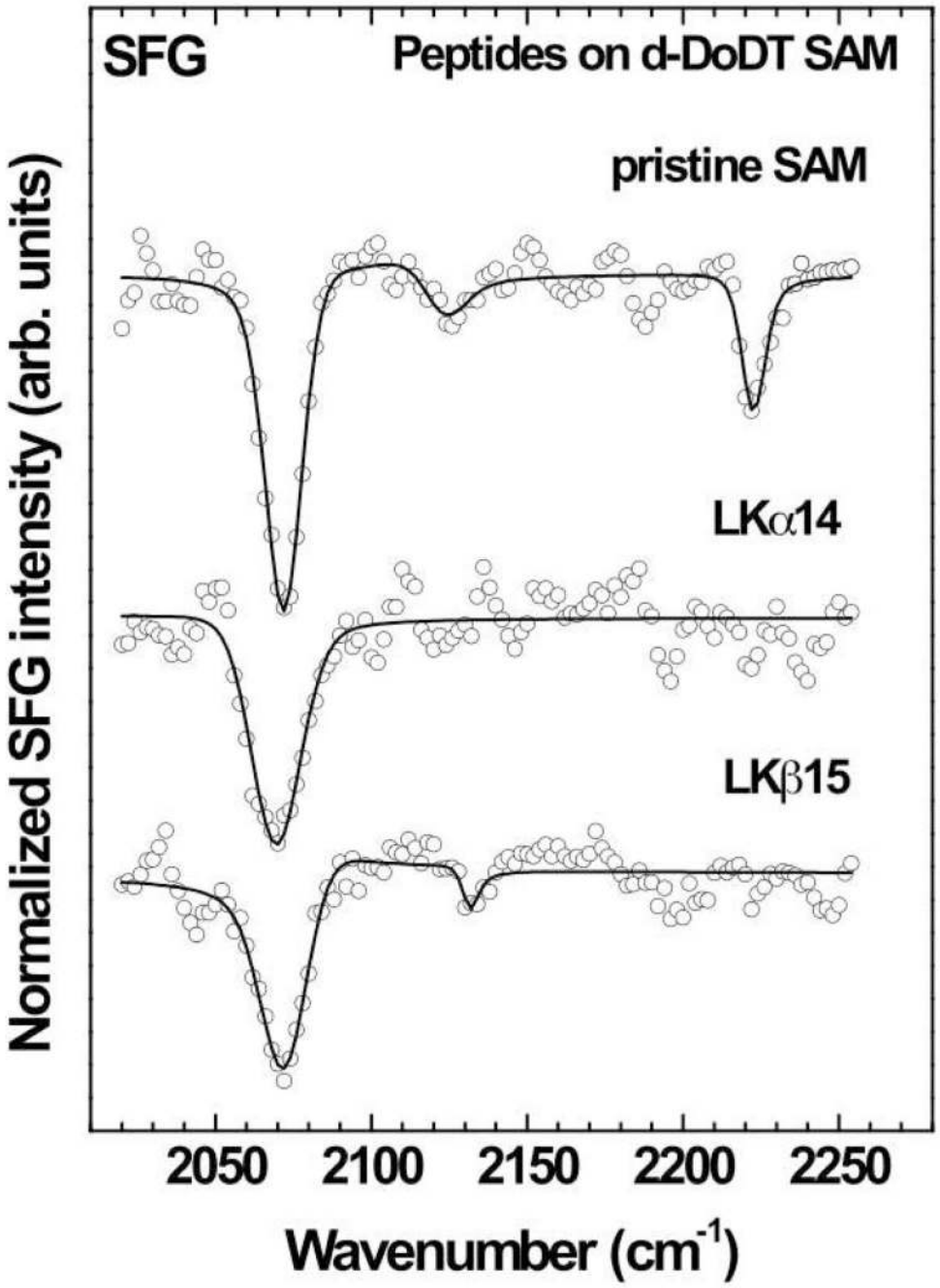

Figure 5.
SFG CD region spectra of pristine and peptide covered deuterated dodecanethiol SAMs. Peaks related to the symmetric and asymmetric stretches of the terminal CD_3 groups of the SAM are detected.

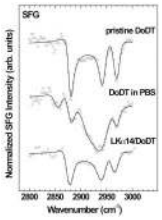

Figure 6.

SFG spectra of pristine DoDT SAMs and DoDT SAMs exposed to either pure PBS or $LK\alpha_{14}$ in PBS at 37° C for 2 h. Resonances related to gauche defects in the aliphatic chain are detected after soaking the DoDT SAMs in pure PBS, but not after soaking the DoDT SAMs in PBS solutions that contained $LK\alpha_{14}$.

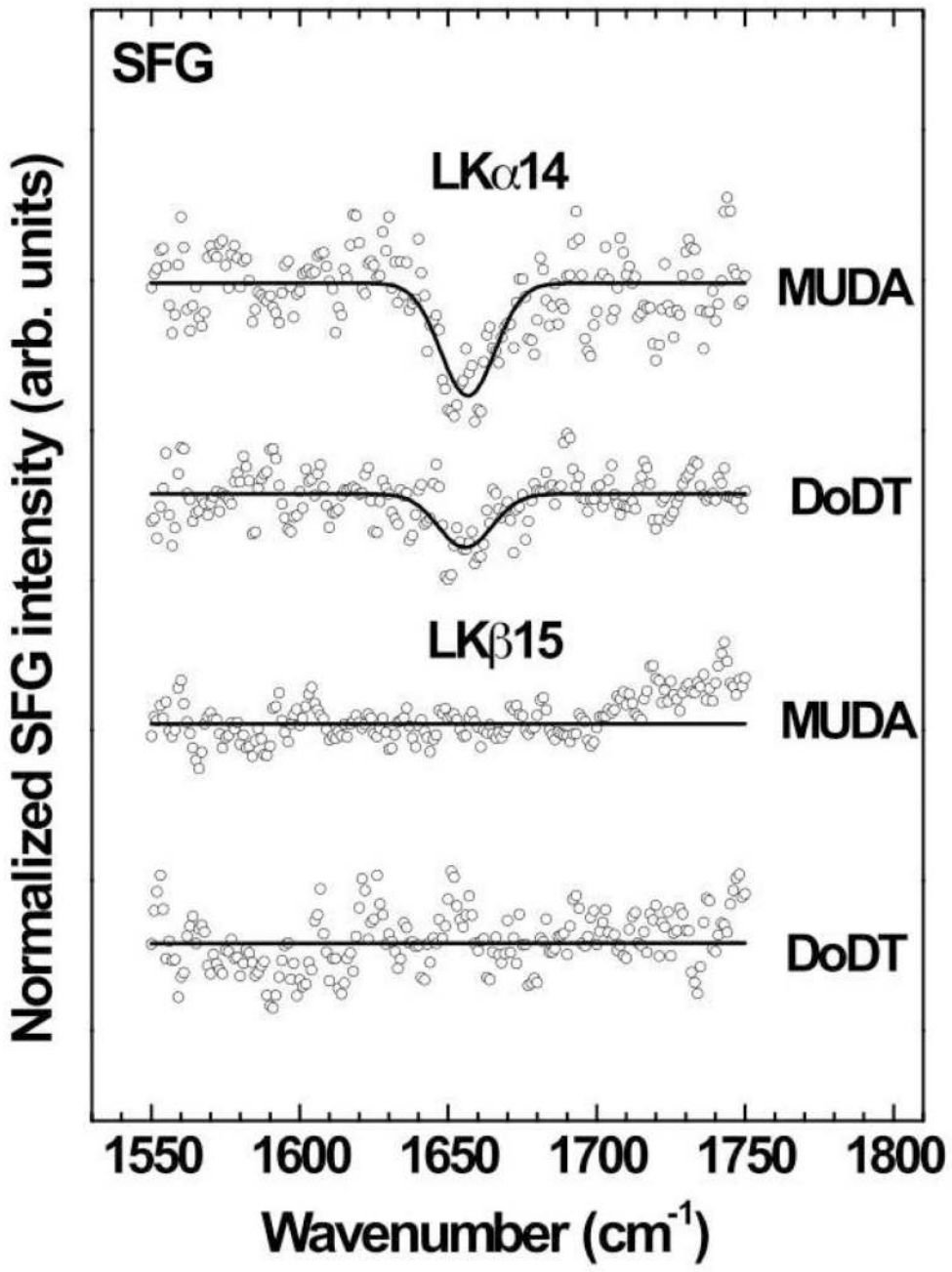

Figure 7.
Amide I region SFG spectra of $LK\alpha_{14}$ and $LK\beta_{15}$ peptides adsorbed onto dodecanethiol (DoDT) and mercaptoundecanoic acid (MUDA) SAMs (circles) along with least-square fits (solid line).

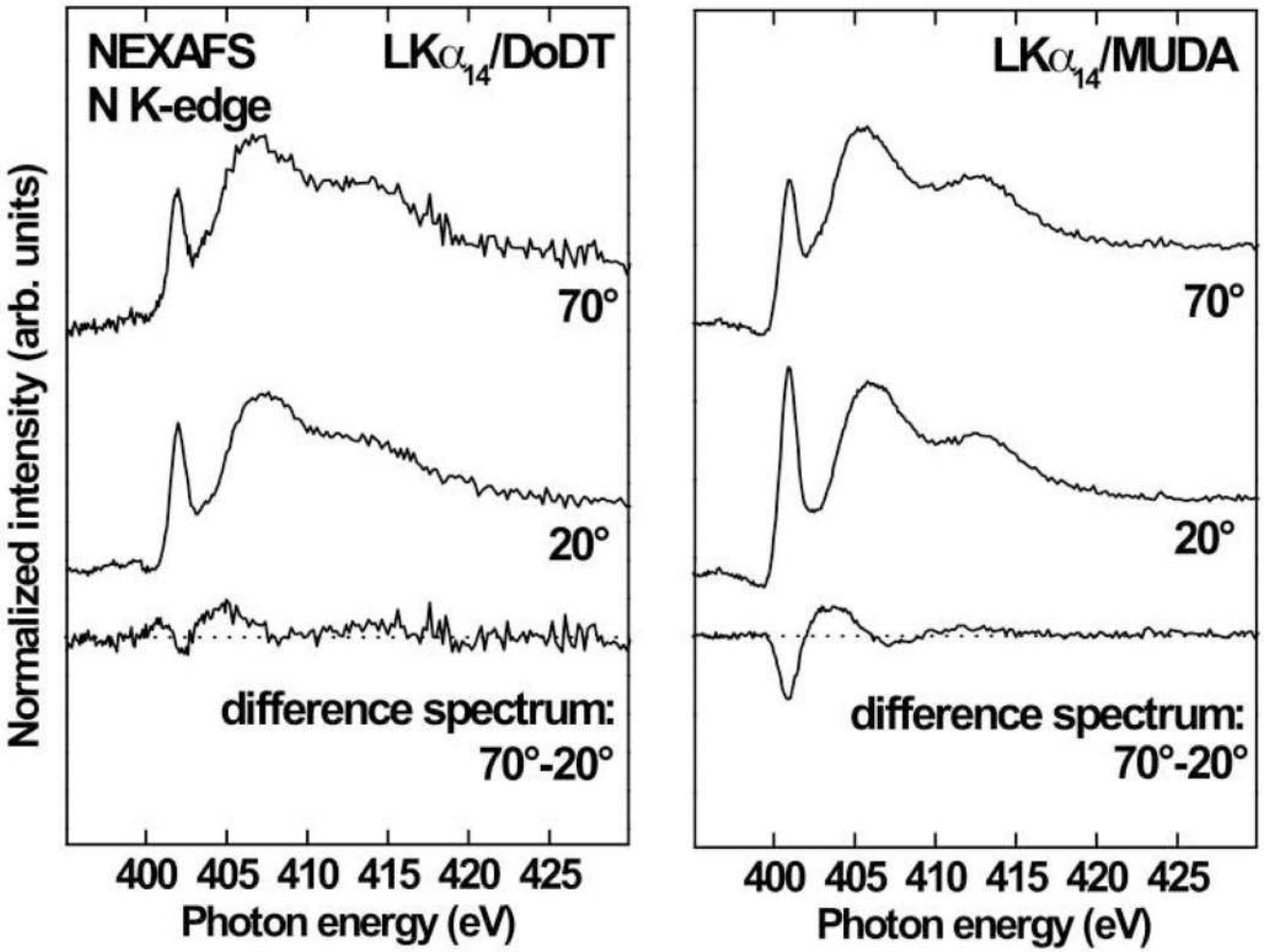

Figure 8.
NEXAFS nitrogen *K*-edge spectra for LKα_{14} adsorbed onto DoDT and MUDA SAMs acquired at a near-normal angle of 70° and at a glancing angle of 20°. The difference spectra between the 70° and the 20° data is also shown.

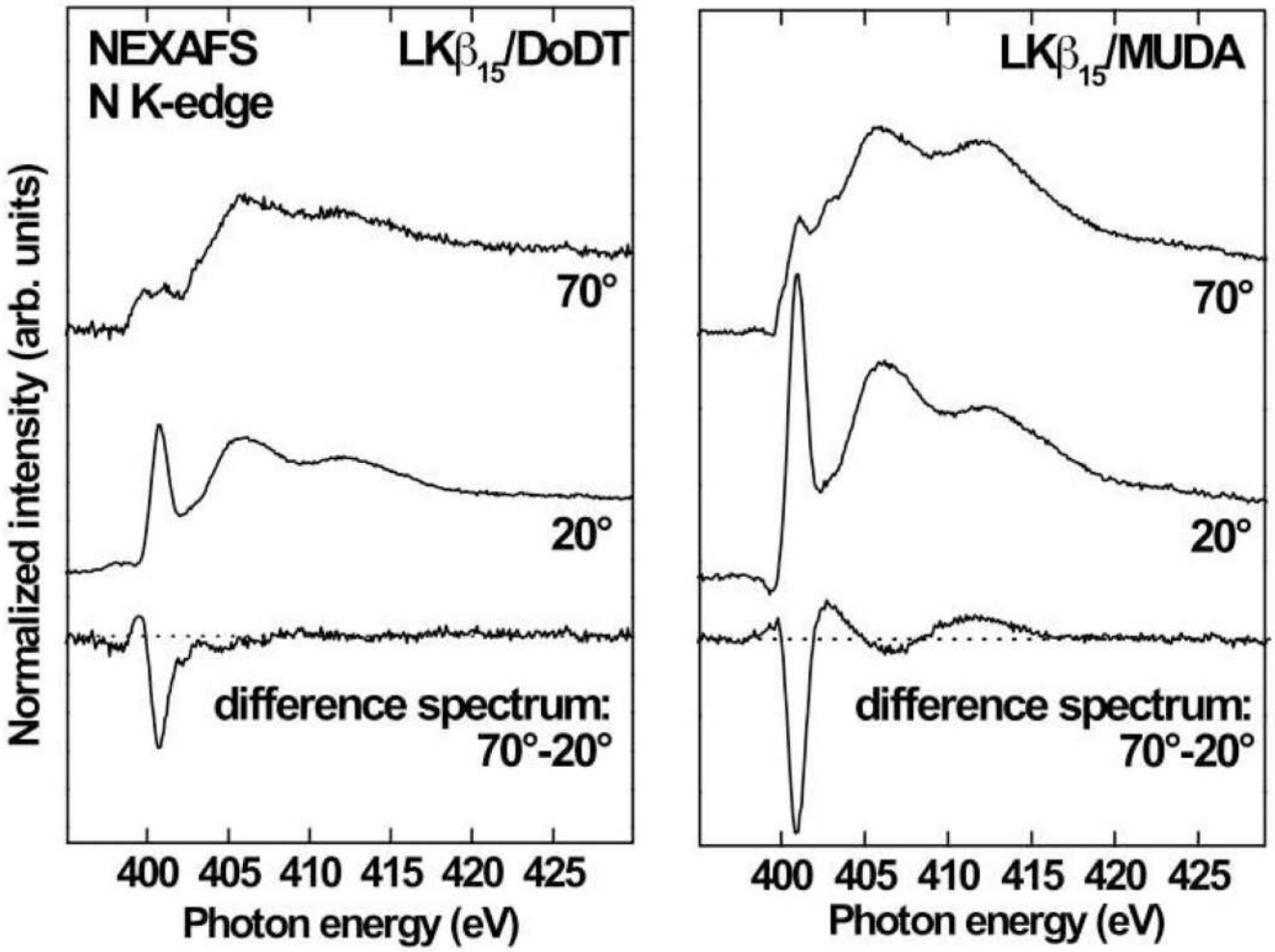

Figure 9.
NEXAFS nitrogen *K*-edge spectra for $LK\beta_{15}$ adsorbed onto DoDT and MUDA SAMs acquired at a near-normal angle of 70° and at a glancing angle of 20°. The difference spectra between the 70° and the 20° data are also shown.

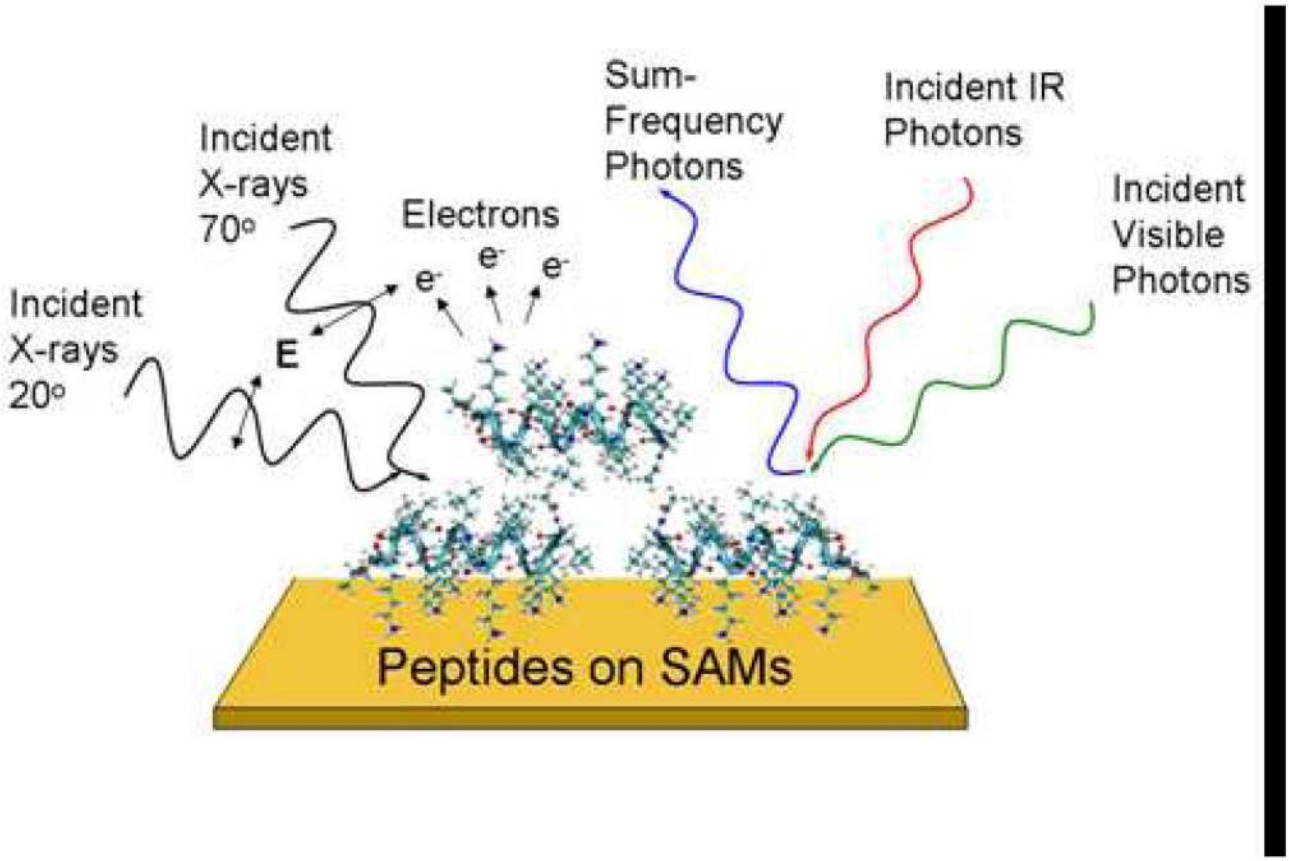

Figure 10.

Table 1

Parameters for peak fits to the SFG spectra of the MUDA and DoDT SAMs, as well as the α-helix and β-strand LK peptides adsorbed onto those SAMs

Film	Frequency (cm^{-1})	Intensity (a.u.)	Realive Phase (rad)
MUDA			
ν_s (CH_2), d^+	2859	0.106	1.81
ν_{as} (CH_2), d^-	2931	0.244	1.81
LKα_{14}/MUDA			
ν_{as} (CH_3), r^-	2966	0.150	1.36
$\nu_{s\ Fermi}$ (CH_3), r^+FR	2937	0.081	1.36
ν_{as} (CH_2), d_ω^-	2907	0.064	1.36
$\nu_{s\ Fermi}$ (CH_2), r^+FR	2891	0.052	1.36
ν_s (CH_3), r^+	2876	0.164	1.36
ν(C=O)	1657	0.995	1.57
LKβ_{15}/MUDA			
ν_{as} (CH_3), r^-	2965	0.095	1.56
$\nu_{s\ Fermi}$ (CH_3), r^+FR	2941	0.117	1.56
ν_{as} (CH_2), d_ω	2912	0.077	1.56
$\nu_{s\ Fermi}$ (CH_2), r^+FR	2888	0.056	1.56
ν_s (CH_3), r^+	2875	0.123	1.56
LKα_{14}/d-DoDT			
ν_{as} (CH_3), r^-	2962	0.177	0.07
$\nu_{s\ Fermi}$ (CH_3), r^+FR	2935	0.039	0.07
ν_s (CH_3), r^+	2873	0.129	0.07
ν(C=O)	1656	0.078	1.57
LKβ_{15}/d-DoDT			
ν_{as} (CH_3), r^-	2962	0.040	0.00
$\nu_{s\ Fermi}$ (CH_3), r^+FR	2938	0.031	0.00
ν_s (CH_3), r^+	2872	0.128	0.00